Dynamic surface wettability of three-dimensional graphene foam*

Huang Wen-Bin(黄文斌)[a], Wang Guang-Long(王广龙)[a], Gao Feng-Qi(高凤岐)[a], Qiao Zhong-Tao(乔中涛)[a], Wang Gang(王 刚)[b], Chen Min-Jiang(陈闽江)[b], Tao Li(陶 立)[b], Deng Ya(邓 娅)[b], and Sun Lian-Feng(孙连峰)[b]†

[a] *Institute of Nanotechnology and Microsystems, Mechanical Engineering College, Shijiazhuang* 050003, *China*
[b] *National Center for Nanoscience and Technology, Beijing* 100190, *China*

(Received 21 August 2013; revised manuscript received 9 October 2013; published online 20 February 2014)

In this work, three-dimensional graphene foams (GFs) are synthesized and characterized by scanning electron microscope (SEM) and Raman spectroscopy. The SEM images indicate that after the growth of graphene, the graphene covers the surface of nickel (Ni) foam uniformly. Raman spectra show that the percentages of monolayer, bilayer, trilayer, and multilayer graphenes are ∼ 58%, ∼ 32%, ∼ 8%, and ∼ 2%, respectively. The contact angle (CA) (∼ 12°) of water droplet (3 μL) on GF is found to be larger than that on Ni foam (∼ 107°), indicating that graphenes have changed the surface wettability of the Ni foam. Meanwhile, the dynamic characteristics of CA of water droplet on GF are different from those on Ni foam. The mechanisms for different behaviors are discussed, which are attributed to volatilization and seepage of water droplets.

Keywords: graphene foam, CVD, surface wettability, contact angle

PACS: 68.08.De, 68.35.Ja, 81.15.Gh **DOI:** 10.1088/1674-1056/23/4/046802

1. Introduction

Graphene, a two-dimensional (2D) crystal with carbon atoms arranged in a hexagonal structure,[1] has attracted extensive attention since it was experimentally discovered through separating the one-atom-thick planar sheet from graphite in 2004.[2] It has many fascinating properties, including giant electron mobility,[3] extremely high thermal conductivity,[4] and large surface areas.[5] These fundamentally superior qualities make it a promising material for a wide range of applications, such as field-effect devices,[6] microelectronic device,[7,8] chemical and biological sensors,[9] etc. To take full advantage of the outstanding characteristics of graphene, it is necessary to integrate individual 2D graphene sheets into a macroscopic structure. However, the integrated structure has poor electrical conductivity because of the high inter-sheet junction contact resistance of graphene sheets.[10]

Therefore, this has become an urgent issue to fabricate large-scale graphene. Macro-porous carbon films were recently fabricated using the 'breath-figure' method, but the method was time-consuming due to the multi-step processing and needed high-temperature reduction and transfer processes.[11,12] Ahn *et al.*[13] achieved the self-assembled foam-like graphene networks through nucleate boiling. However, some properties of graphene synthesized by the methods above were less favorable for those of CVD-grown graphene.

The wettability of a solid surface, which has been researched much recently,[14–17] is important for a wide range of applications in industrial settings, including paper and paint industries,[18] biomedical industries for the design of implants and medical devices,[19,20] such as dental implants, contact lenses, the design of biomimetic microfluidic devices, and the determination of solid–liquid adhesion force. So, it is significant to investigate the surface wettability of graphene foams (GF).

In this paper, GF is synthesized by CVD firstly. GF is characterized by scanning electron microscope (SEM) and laser Raman spectroscopy. Then, the surface wettability of GF is investigated, the contact angle (CA) of a water droplet on GF varies with time nonlinearly, but the variation curve is different from that on Ni foam, indicating that the graphene has affected the surface wettability of Ni foam. The volume of a water droplet on GF deceases gradually, which is attributed to volatilization and the seepage of water into the porous structure of the GF.

2. Experiment

2.1. Synthesis of GF

The GF was synthesized on a scaffold of Ni foam (1.5 cm × 1.5 cm × 0.5 cm) by CVD,[21,22] a schematic diagram of the apparatus used is shown in Fig. 1(a). The Ni foam was placed in a round quartz tube, which was inserted into the horizontal tube furnace (∼ 32-mm inner diameter). A transition tube was used to link the air inlet end and the furnace, whose inner diameter was ∼ 6 mm. Carbon atoms were deposited on the Ni foam through CH_4 decomposition at ∼ 1000 °C under ambient pressure.[23] After growing for about 10 minutes, a continuous

*Project supported by the National Natural Science Foundation of China (Grant Nos. 10774032 and 90921001) and the Key Knowledge Innovation Project of the Chinese Academy of Sciences on Water Science Research, Instrument Developing Project of the Chinese Academy of Sciences (Grant No. Y2010031).

†Corresponding author. E-mail: slf@nanoctr.cn

© 2014 Chinese Physical Society and IOP Publishing Ltd

GF was formed as a macroscopic structure with extremely thin interconnected graphene sheets outside the Ni foam.

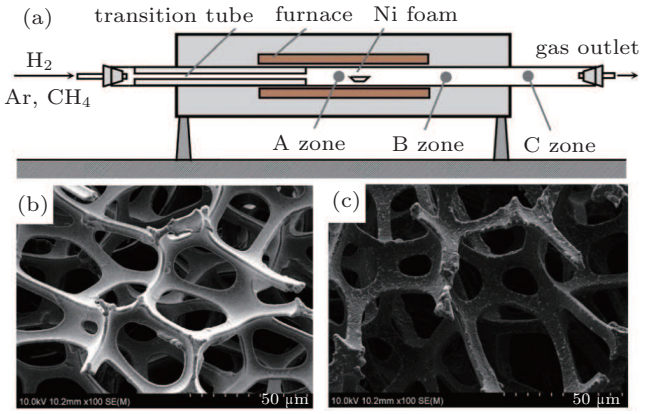


Fig. 1. (color online) Schematic diagram of the apparatus used for synthesizing GF (a), SEM images of Ni foam (b), and GF (c).

2.2. Characterization of GF

SEM is a powerful tool for investigating the characteristics of materials. The SEM images (100 ×) of Ni foam and GF, which are shown in Figs. 1(b) and 1(c), were captured by a Hitachi S4800.

Raman spectroscopy (Renishaw in Via Raman Spectroscope)[24,25] is one of the most common characterization tools in graphene research. The Raman spectra of our samples were collected using the laser excitation of ∼ 514 nm by an argon ion laser. To avoid damage to the samples, we set the laser power to be less than 1 mW. A ∼ 1 μm laser spot size was obtained with using a 100× objective lens with a numerical aperture of 0.926.

2.3. Measurements of CA and volume

To investigate the surface wettability of GF, the CA and volume of a distilled water droplet (3 μL) were measured by sessile-drop method[26,27] on a Dataphysics OCA20 CA system at room temperature. Firstly, a drop of liquid was deposited with a micro-syringe onto the dry GF in air. Images of the drops were captured, and the experimental profile of each drop was extracted. Then, the three-phase contact points were identified, which was a highly delicate process. The Young–Laplace theoretical model[28] based on axisymmetric drop shape analysis was selected and the tangent line of the goniometer was adjusted to the contact points to obtain the CA automatically. This technique often resolves CAs with an accuracy of ∼ 0.2°. The volume of liquid was also calculated using the same theoretically calculated model by an automatic computer image recognition technique.

3. Results and discussion

The Raman spectrum of graphene is dominated by two prominent features:[29] G band and 2D band. By combining the intensity images of the G and the 2D bands, one can reliably estimate the number of graphene layers.[30,31] As shown in Fig. 2(a), there are typical Raman spectra of GF. From bottom to top, the intensity ratios of the 2D to G modes (I_{2D}/I_G) of the as-grown GF show that the walls of GF are comprised of monolayer, bilayer, trilayer, and multi-layer graphene sheets. The strongly-suppressed defect-related D band confirms high quality graphene grown by CVD. In the analysis, the I_{2D}/I_G of 49 points among all 50 counted ones lie between 1.5 and 3.0, indicating that ∼ 98% of them are covered by monolayer, bilayer, and trilayer graphene. The histogram of the layers of GF samples is shown in Fig. 2(b).

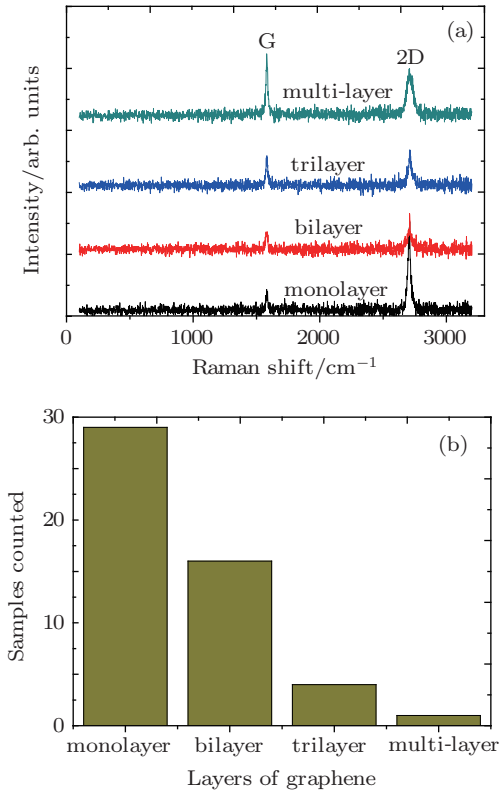


Fig. 2. (color online) Raman spectra (a) and histogram of layers (b) of GF.

The surface wettability of an ideally flat, homogeneous, and inert surface can be described by CA, which can be expressed by Young's equation as follows:[32,33]

$$\cos\theta = (\gamma_{sv} - \gamma_{sl})/\gamma_{v}, \tag{1}$$

where θ denotes the CA of a droplet deposited on a surface, that is, at a position where the solid, liquid, and vapor phases are in contact, considering a balance between liquid–vapor (γ_{lv}), solid–liquid (γ_{sl}), and solid–vapor (γ_{sv}) interfacial tensions.

Figures 3(a) and 3(b) show the cross-sectional views of water droplets lying on the surfaces of Ni foam and GF at three different moments: 0 s, 500 s, and 1000 s. At 0 s, the CA of water droplet lying on GF is ∼ 126°, which is larger than that

on Ni foam. So, we can obtain the conclusion that graphene can affect the surface wettability of Ni foam. From Fig. 3(b), we can obtain that the CA decreases to $\sim 85^\circ$ after 500 s and $\sim 30^\circ$ after 1000 s, the CA of water droplet becomes smaller and smaller with time going by. The same conclusion can be drawn from Fig. 4(a), in which the variation curves of CAs of water droplets on Ni foam and GF are shown.

As the CA varies with time, the volume of water droplet on GF keeps decreasing as shown in Fig. 3(b), the volumes of water droplet are 3 mL, 1.4 mL, and 0.2 mL at three different moments: 0 s, 500 s, and 1000 s. To explore the causes of the phenomenon, we set up two different contrast experiments, in which Ni foam and a piece of Ni are used as substrates, as shown in Figs. 3(a) and 3(c). Obviously, during the same period (0 s $\sim$ 500 s), the volume variable quantity of water droplet on Ni foam is larger than that on Ni, indicating that the volatilization is not the only cause for the volume variation. So, we can infer that the porous structure of Ni foam and GF plays a role in the volume variation and some of water has seeped into the pores of the porous materials.

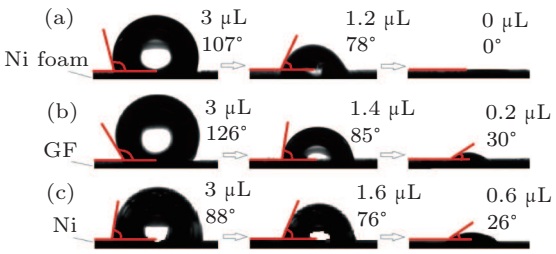


Fig. 3. (color online) Cross-sectional views of water droplet on Ni foam (a), GF (b), and a piece of Ni (c), the volumes and CAs at three different moments (0 s, 500 s, and 1000 s) are shown.

To compare the volatilization rate of water droplets on Ni foam with that on GF, and explore the deeper causes of the phenomenon above, we need to consider the Kelvin formula[34], as follows:

$$\frac{p_r - p_0}{p_0} = \frac{2\gamma M}{RTR'\rho}, \tag{2}$$

where p_r is the vapor pressure of water droplet, p_0 is the common vapor pressure, γ is the surface tension of water, M is the molar mass of water droplet, R is the gas constant, T is the environmental temperature, and is expressed on an absolute temperature scale (K), R' is the radius of curvature, and ρ is the density of water. From the above formula it follows that the smaller the curvature radius of water droplet, the larger the vapor pressure of water droplet is.

By comparing Fig. 3(a) with Fig. 3(b), it can be easily inferred that the curvature radius of water droplet on GF is smaller than that on Ni foam, and the water droplet on GF should decrease more quickly. However, an opposite conclusion is drawn from Fig. 3, which should be attributed to the existence of graphene. As shown in Fig. 4(b), three curves with different colors reflect the variations of volumes of water droplets on Ni foam (red line), GF (black line), and Ni (green line) with time. The same conclusion can be drawn from Fig. 3, that is, the volume of water droplet on Ni foam decreases more quickly than that on Ni due to the porous structure, the volume of water droplet on GF decreases more slowly than that on Ni foam due to graphene.

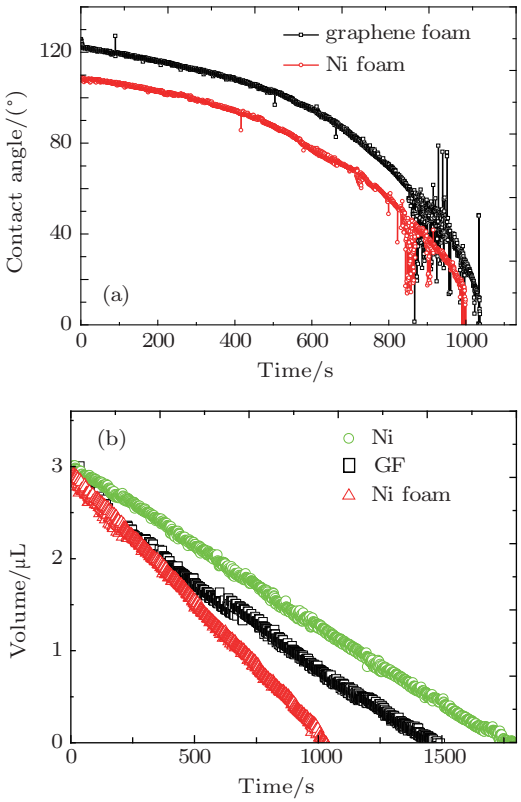


Fig. 4. (color online) (a) Time variations of CAs of water droplets on Ni foam (red line), graphene foam (black line), and (b) time variations of volumes of water droplets on Ni foam (red line), GF (black line), and Ni (green line).

From Figs. 1(b) and 1(c), we know that the pore size of Ni foam has little difference from that of GF. So the variation rate of water droplet on GF is not influenced by the pore size, but by the three-dimensional graphene itself. As reported before, graphene as a single-atom-thick sheet composed of sp^2 hybridized carbon atom is highly hydrophobic.[35] Therefore, both the larger CA (0 s) and slower variation rate of water droplet on GF than on Ni foam are attributed to the hydrophobic characteristics of graphene.

4. Conclusion

In this paper, we synthesized GF by CVD in growth chamber firstly. Then, GF was characterized by SEM and laser Raman spectroscopy, and it is concluded that $\sim 98\%$ of the GFs are monolayer, bilayer, and trilayer. As a continuous macroscopic structure, GF overcomes the low quality and/or

high inter-sheet junction contact resistance of integrated structures of graphene sheets.

In order to investigate the surface wettability of GF, the CA of water droplet (3 μL) on GF is measured, which is found to be larger than that on Ni foam, indicating that graphene has changed the surface wettability of Ni foam. The volume of a water droplet on GF is reduced gradually, which is attributed to volatilization and seepage into its pores. However, the reducing rate of water droplet on GF is slower than that on Ni foam due to the existence of graphene.

Acknowledgment

The authors sincerely thank the National Center for Nanoscience and Technology, Institute of Nanotechnology and Microsystems for providing a fine work environment, experimental facility, and technical support.

References

[1] Weiss N O, Zhou H L, Liao L, Liu Y, Jiang S, Huang Y and Duan X F 2012 *Adv. Mater.* **24** 5782
[2] Novoselov K S, Geim A K, Morozov S V, Jiang D, Zhang Y, Dubonos S V, Grigorieva I V and Firsov A A 2004 *Science* **306** 666
[3] Geim A K and Novoselov K S 2007 *Nat. Mater.* **6** 183
[4] Balandin A A 2008 *Nano Lett.* **8** 902
[5] Niyogi S 2006 *J. Am. Chem. Soc.* **128** 7720
[6] Luo Z T, Lu Y, Somers L A and Johnson A T C 2009 *J. Am. Chem. Soc.* **131** 898
[7] Yin J, Zhang Z H, Li X M, Zhou J X and Guo W L 2012 *Nano Lett.* **12** 1736
[8] Wu H Q, Linghu C Y, Lü H M and Qian H 2013 *Chin. Phys. B* **22** 098106
[9] Lu C H, Yang H H, Zhu C L, Chen X and Chen G N 2009 *Angew. Chem. Int. Ed.* **121** 4879
[10] Chen Z P, Ren W C, Gao L B, Liu B L, Pei S F and Cheng H M 2011 *Nat. Mater.* **10** 424
[11] Lee S H 2010 *Angew. Chem. Int. Ed.* **122** 10282
[12] Yin S Y, Zhang Y Y, Kong J H, Zou C J, Li C M, Lu X H, Ma J, Boey F Y C and Chen X D 2011 *ACS Nano* **5** 3831
[13] Ahn H S, Jang J W, Seol M, Kim J M, Yun D J, Park C, Kim H, Youn D H, Kim J Y, Park G, Park S C, Kim J M, Yu D I, Yong K, Kim M H and Lee J S 2013 *Sci. Rep.* **396** 1
[14] Yuan Q Z and Zhao Y P 2010 *Phys. Rev. Lett.* **24** 104
[15] Mei M F, Yu B M, Luo L and Cai J C 2010 *Chin. Phys. Lett.* **27** 076802
[16] Gong M G, Liu Y Y and Xu X L 2010 *Chin. Phys. B* **19** 106801
[17] Guo H K and Fang H P 2005 *Chin. Phys. Lett.* **22** 787
[18] Atefi E, Mann J A and Tavana H 2013 *Langmuir* **4** 17
[19] Menzies K L and Jones L 2010 *Optom. Vision Sci.* **87** 387
[20] Aguilar-Mendoza J A, Rosales-Leal J I, Rodriguez-Valverde M A, Gonzalez-Lopez S and Cabrerizo-Vilchez M A 2008 *Dent. Mater.* **24** 994
[21] Chen W, Fan Z L, Zeng G F and Lai Z P 2013 *Journal of Power Sources* **225** 251
[22] Wang W R, Liang C and Li T 2013 *Chin. Phys. B* **22** 028102
[23] Yan Z, Peng Z W, Sun Z Z, Yao J, Zhu Y, Liu Z, Ajayan P M and Tour J M 2011 *ACS Nano* **5** 8187
[24] Yang H C, Chen M J, Zhou H Q, Qiu C Y, Hu L J, Yu F, Chu W G, Sun S Q and Sun L F 2011 *J. Phys. Chem. C* **115** 16844
[25] Wu M H, Li X, Pan D, Liu L, Yang X X, Xu Z, Wang W L, Sui Y and Bai X D 2013 *Chin. Phys. B* **22** 086101
[26] Yu F, Hu L J, Zhou H Q, Qiu C Y, Yang H C, Chen M J, Lu J L and Sun L F 2013 *Journal of Nanoscience and Nanotechnology* **13** 1335
[27] Shi Z M, Dong J H and Ma W 2012 *Adv. Mater. Res.* **602** 1735
[28] Mettu S and Chaudhury M K 2012 *Langmuir* **28** 14100
[29] Malard L M, Pimenta M A, Dresselhaus G and Dresselhaus M S 2009 *Phys. Rep.* **473** 51
[30] Dong J, Yao Z H, Yang T Z, Jiang L L and Shen C M 2013 *Sci. Rep.* **1733** 1
[31] Papadopoulos P, Mammen L, Deng X, Vollmer D and Butt H J 2012 *Chem. Lett.* **41** 1343
[32] Korhonen J T, Huhtamaki T, Ikkala O and Ras R H A 2013 *Langmuir* **29** 3858
[33] Yu Y S 2012 *Appl. Math. Mech.* **33** 1025
[34] Camuffo D 1984 *Water, Air, and Pollution* **21** 151
[35] Zha D A, Mei S L, Wang Z Y, Li H J, Shi Z J and Jin Z X 2011 *Carbon* **49** 5166